

Development and study of methods for estimating retinal vessel parameters using a modified local fan transform

N.Yu. Ilyasova^{1,2}, A.S. Baisova¹, A.V. Kupriyanov^{1,2}

¹Samara National Research University, 34 Moskovskoe Shosse, 443086, Samara, Russia

²Image Processing Systems Institute – Branch of the Federal Scientific Research Centre “Crystallography and Photonics” of Russian Academy of Sciences, 151 Molodogvardeyskaya st., 443001, Samara, Russia

Abstract

Estimation of the geometric parameters of blood vessels is an important stage in the diagnosis of many cardiovascular diseases. In this work, we describe a method for estimating the diameter of blood vessels based on a modified local fan transform. We present experimental results that show in which way the accuracy of blood vessel estimation is affected by the noise-to-signal ratio in the image under analysis, vessel curvature radius, and the number of points and angles over which the averaging is done. The method is experimentally shown to be immune to various types of noise, structural complexity of the object, and variations in the vessel curvature radius.

Keywords: local fan transform; eye fundus; vascular image processing; local parameter estimation

1. Introduction

Early detection, analysis, and timely treatment of eye pathologies are critical in the prevention of eye-sight loss. Automatic detection and classification of eye diseases have recently become an important area of research, showing a tremendous potential for the early treatment of eye diseases [1, 2].

Glaucoma is a severe pathology of the eye which can be diagnosed by analyzing the state of the optic disk, or more precisely, the relationship between vascular parameters of different areas. By studying the derived information, the eye image can be classified as normal or containing a pathology. In a most quick way, the pathology can be detected by estimating the blood vessel width [3, 4]. According to modern data, the deviation of the diameter of a pathological vessel from a normal one is just about 20%. This fact is a major motivation behind the development of most precise methods for estimating the retinal arterioles.

The vascular disease is diagnosed using diagnostic features based on the geometric parameters of vessels. Among most important parameters are the vessel's diameter and direction.

Recent years have seen the development of many image processing algorithms aimed at analyzing both the vascular system in general and the optic disk, in particular. The algorithms use different approaches and have their benefits and shortcomings [5-12]. The algorithms based on a complex continuous wavelet-transform [12] are best suited for describing the structure of lines in different directions. A method for estimating vascular parameters proposed in [13] relies on mathematical morphology as an instrument for extracting image fragments suitable for the description of boundaries and skeleton of a vessel. The method utilizes a sparse representation of signals. In [13], each signal is assumed to be composed of a linear combination of several morphologically different components. The final map of a vessel is constructed using an adaptive threshold method. The method was shown to perform well in detecting anomalies and pathologies in the retina image. When used on their own, a major disadvantage of the morphological techniques is that they disregard the information on the vessel profile shape. Besides, while searching just for elongated structures, heavily twisted vessels can be missed out.

A method for estimating the vessel diameter using an algorithm based on a parametric model of an arbitrarily complex-shaped vessel was reported in Ref. [14]. The automatic algorithm is capable of segmenting the entire vascular tree, calculating vessel's diameter and direction in a digital ophthalmologic image. An algorithm that utilizes a new parametric surface model of the vessel intensity profile was described in Ref. [15]. Compared to other methods, the said method offers an advantage of robustness, whereas, as the authors mention, on the negative side is the dependence of the results on the test data and experimental conditions. If vessel diameters in the test data vary in a wide range, the measurement accuracy significantly deteriorates. Other approaches to measuring the diameter of vessels rely upon the approximation of the vessel brightness profile. With the vessel brightness normally having a Gaussian profile, a Gaussian curve is often used to approximate the vessel cross-section [16, 17]. However, with the diseased vessels tending to have well pronounced boundaries, their profile looks like a combination of two Gaussians, making it difficult to measure their diameter in an automatic mode and creating a possibility to falsely recognize a single vessel as two ones.

In this work, we propose a method for estimating local parameters of a fundus vascular system that exploits a modified fan transform, which is more noise-immune thanks to the additional filtering and noise averaging. Another advantage is that the method can perform a high-efficiency analysis of bifurcations, crossovers, and termination of vessels in the presence of interfering factors, such as close vessels.

2. A modified local fan transform

We introduce a modified local fan transform (MLFT) intended to operate with real-life low-quality vascular network imagery, which is well suited for processing images characterized by spots and closely spaced vessels.

With this method, the brightness distribution function is analyzed sector-wise depending on the sector's radius, size, and rotation angle (Fig. 1a) [2]. For each sector's position, the following local parameters are calculated: the average value and

variance of the brightness function $f(x, y)$. By analyzing these parameters as a function of angle, it is possible to detect the vessel in a given point, estimating its width and direction.

A modified LFT is defined by the following formulae:

$$F(x_0, y_0, a, q, r) = \frac{1}{S_q} \int_0^{a+q/2} \int_0^r f(x_0 + t \cos j, y_0 + t \sin j) dt dj, \tag{1}$$

$$D(x_0, y_0, a, q, r) = \frac{1}{S_q} \int_0^{a+q/2} \int_0^r [f(x_0 + t \cos j, y_0 + t \sin j) - F(x_0, y_0, a, q, r)]^2 dt dj, \tag{2}$$

where (x_0, y_0) is a point of measurement, a is a polar angle, q is a solid angle of the sector, r is the radius, and $S_\theta = \theta R^2/2$ is the sector's area.

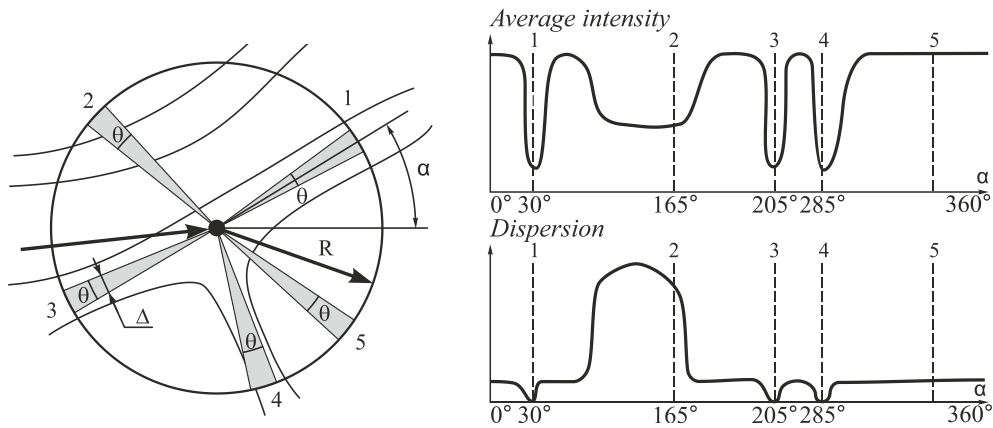


Fig. 1. A circular region with differently oriented sector.

3. Estimating the local direction of a vessel

The MLFT-aided method enables a local vessel direction to be evaluated. When compared with the LFT-aided approach, the MLFT method enables the radial profile with more pronounced minima to be obtained, with the local minima corresponding to bifurcation directions (Fig. 2).

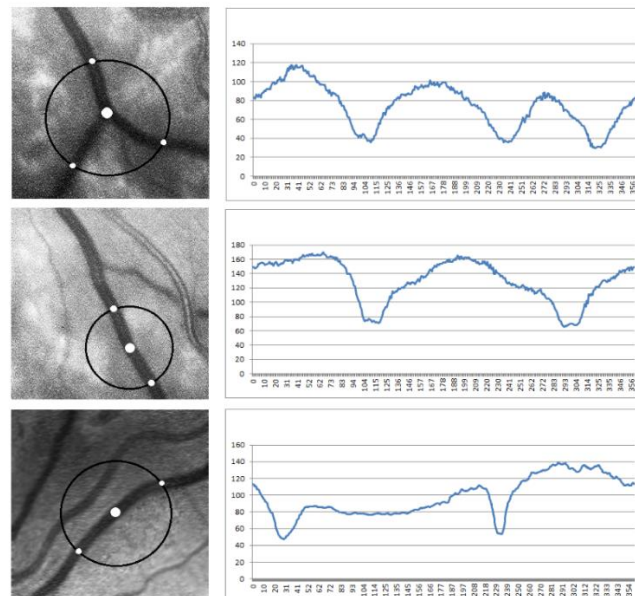


Fig. 2. Vessel fragments with corresponding radial profiles.

Thus, for a vessel direction to be identified, an optimization problem of searching for minima needs to be solved for each angle-dependent radial profile for a specific radius [2]. The algorithm operates by analyzing a list of directions, which represents a vector for each radius, with its length being equal to the number of directions and its magnitude taking a unit value if a bifurcation is detected and being zero otherwise. The list of directions may contain regions of constant values equal to unity.

This is the indication of detecting a bifurcation with larger-than-pixel width. In this case, the unit value is taken just at the central region's pixel.

4. Estimating the vessel width

The vessel width will be evaluated using an LFT and on the assumption that the vessel is in parallel with the Ox -axis (Fig. 3).

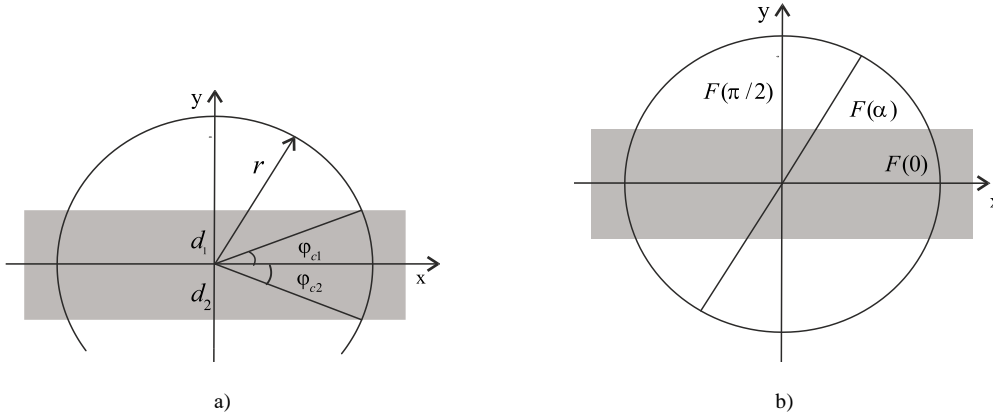


Fig. 3. Horizontal vessel section.

The fan transform of Eq. (1) can be analytically calculated at point (x_0, y_0) at $\theta=0$ (Fig. 3a):

$$F_f(\alpha, r) = \left(r - \frac{d_1}{\sin \alpha} \right) f_0 + \frac{d_1}{\sin \alpha} f_1,$$

where f_0 is the background brightness, f_1 is the vessel brightness, d_1, d_2 are width components with respect to the axis, $\alpha \in (\varphi_{c1}, \pi - \varphi_{c2})$, $\varphi_{c1} = \arcsin \frac{d_1}{r}$, $\varphi_{c2} = \arcsin \frac{d_2}{r}$. In the general case:

$$F(\alpha, r) = \begin{cases} (r - d_1/\sin \alpha) f_0 + f_1 d_1/\sin \alpha, & \alpha \in (\varphi_{c1}, \pi - \varphi_{c1}) \\ (r - d_2/\sin(\alpha - \pi)) f_0 + f_1 d_2/\sin(\alpha - \pi), & \alpha \in (\varphi_{c2}, \pi - \varphi_{c2}) \\ r f_1, & \alpha \in (0, \varphi_{c1}) \cup (\pi - \varphi_{c1}, \pi + \varphi_{c2}) \cup (2\pi - \varphi_{c2}, 2\pi) \end{cases}$$

Let us analyze a set of equations (Fig. 3b):

$$\begin{cases} F(0, r) = 2r f_1 \\ F(\pi/2, r) = (2r - d) f_0 + d f_1 \\ F(\alpha, r) = (2r - d/\sin \alpha) f_0 + f_1 d/\sin \alpha, \alpha \in (\varphi_{c \max}, \pi - \varphi_{c \max}), \varphi_{c \max} = \max(\varphi_{c1}, \varphi_{c2}) \end{cases}$$

Here, the angle α is such that the interval of integration intersects both boundaries of the vessel. Hence, the diameter can be evaluated as

$$d = 2r \frac{F_r(\alpha, r) - F_r(\pi/2, r)}{\frac{F_r(0, r) - F_r(\pi/2, r)}{\sin \alpha} - F_r(0, r) + F_r(\alpha, r)} \tag{3}$$

In practice, diameter components d_1, d_2 often need to be evaluated. Given a circular window of radius r and a horizontal vessel, the terms d_1 and d_2 can be described by similar sets of equations:

$$\begin{cases} F(0, r) = r f_1 \\ F(\pi/2, r) = (r - d_1) f_0 + d_1 f_1 \\ F(\alpha_1, r) = (r - d_1/\sin \alpha_1) f_0 + f_1 d_1/\sin \alpha_1, \alpha_1 \in (\varphi_{c1}, \pi - \varphi_{c1}) \end{cases},$$

$$\begin{cases} F(0, r) = r f_1 \\ F(3\pi/2, r) = (r - d_2) f_0 + d_2 f_1 \\ F(\alpha_2, r) = (r - d_2/\sin(\alpha_2 - \pi)) f_0 + f_1 d_2/\sin(\alpha_2 - \pi), \alpha_2 \in (\varphi_{c2} + \pi, 2\pi - \varphi_{c2}) \end{cases}$$

With a real vessel having an arbitrary direction, the algorithm for width estimation is, at first, given the vessel direction defined by an angle a_s , which is preliminarily calculated by the direction algorithm. With a specific value prescribed to the angle, the diameter components are evaluated as

$$d_1 = r \frac{F(a_1 + a_s, r) - F(p/2 + a_s, r)}{\frac{F(0 + a_s, r) - F(p/2 + a_s, r)}{\sin a_1} - F(0 + a_s, r) + F(a_1 + a_s, r)} \tag{4}$$

$$d_2 = r \frac{F(a_2 + a_s, r) - F(3p/2 + a_s, r)}{\frac{F(0 + a_s, r) - F(3p/2 + a_s, r)}{\sin(a_2 - p)} - F(0 + a_s, r) + F(a_2 + a_s, r)} \tag{5}$$

To enhance the accuracy of estimating the diameter components, a value averaged over N_φ different angles will be considered. Below, an estimate for a single diameter component is given:

$$d_1 = \frac{1}{N_\varphi} \sum_{k=1, \varphi_k \in (\varphi_{c1}, \pi - \varphi_{c1})}^{N_\varphi} \left(r \frac{F_f(\varphi_k + \alpha_s, r) - F_f(\pi/2 + \alpha_s, r)}{\frac{F_f(0 + \alpha_s, r) - F_f(\pi/2 + \alpha_s, r)}{\sin \varphi_k} - F_f(0 + \alpha_s, r) + F_f(\varphi_k + \alpha_s, r)} \right)$$

If Eqs. (3) and (5) are employed in a straightforward manner, the components of the ray and fan transforms $F(a, r)$ [2,7,9] taken for a heavily noised vascular image can be calculated with an error, resulting in an incorrectly evaluated vessel's diameter. To avoid this in this work, the values of the LFT are averaged over points located uniformly on the perpendicular line of integration. Figure 4 illustrates the process of averaging three ray transform components.

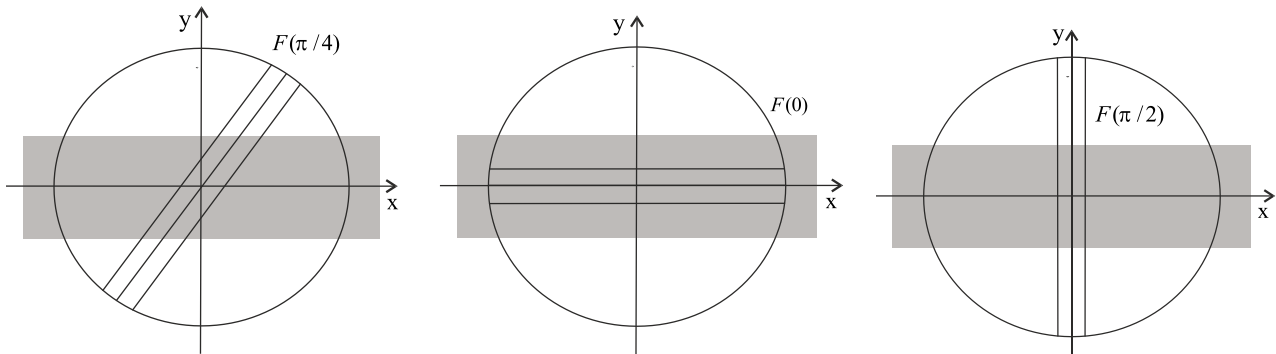


Fig. 4. An example of calculating a LFT using point-wise averaging.

5. Experimental study

We analyzed in which way the accuracy of estimating the vessel diameter depends on the noise-to-signal ratio for additive white noise. Figure 5 shows the relative diameter estimation error as a function of the noise-to-signal ratio: $\varepsilon^2 = \frac{1}{N} \sum_{i=1}^N (\hat{d}_i - d)^2 / d^2$, where \hat{d} is the evaluated diameter, d is the real diameter measured on a test image, and r is supposed to be not smaller than $d/\sin(\pi/3)$.

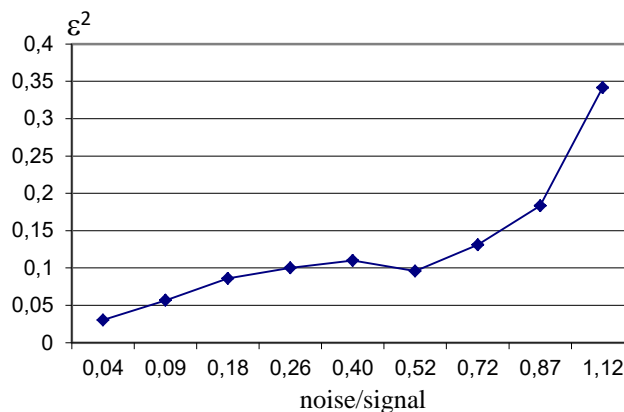


Fig. 5. Error of width estimation vs. the noise-to-signal ratio.

The study conducted on synthetic images has shown the method for estimating local parameters to be immune against the additive noise. For instance, the error of estimating the local diameter was found to be not larger than 8% given the noise-to-signal ratio under 0.25.

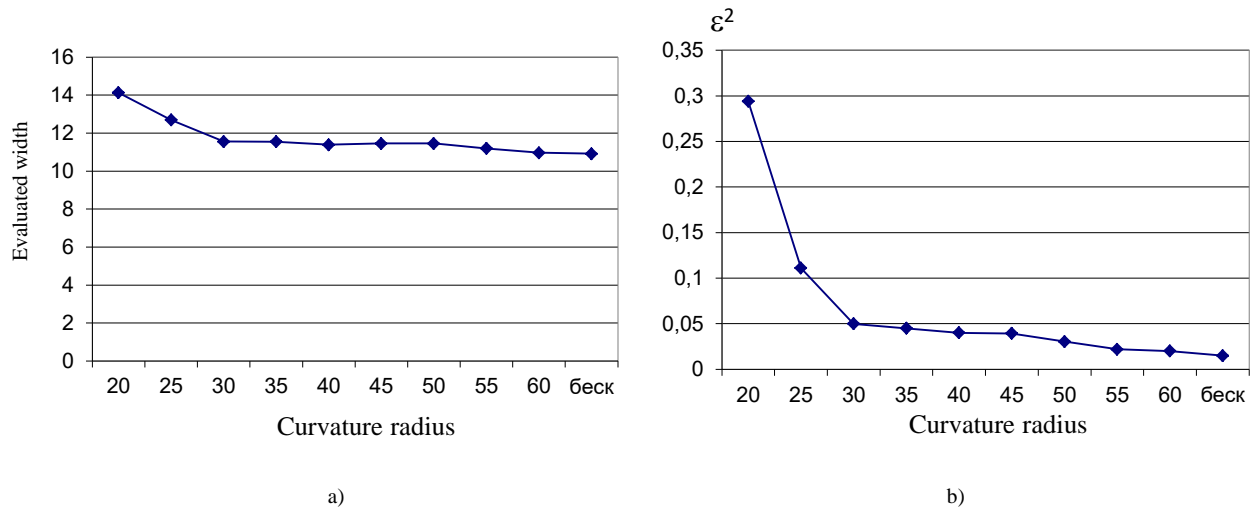


Fig. 6. (a) Evaluated width and (b) estimation error against the curvature radius.

The average vessel diameter estimate as a function of vessel curvature is shown in Fig. 6a. As test vascular images, we utilized the images of an annular sector 11 pixels in width and inner circle radius ranging from 20 to 60 pixels. A same-width straight-line segment (of infinite curvature radius) was also analyzed in order to determine an "estimated width". From the above plots, the error of width determination is seen to increase with increasing vessel curvature. Figure 7 depicts in which way the average vessel diameter estimate depends on the number of averaging points (see section 4, Fig. 4), given the signal-to-noise ratio equal to 25. The experimental results have shown that with the number of averaging points increasing to 13, the error falls from 0.1 till 0.02.

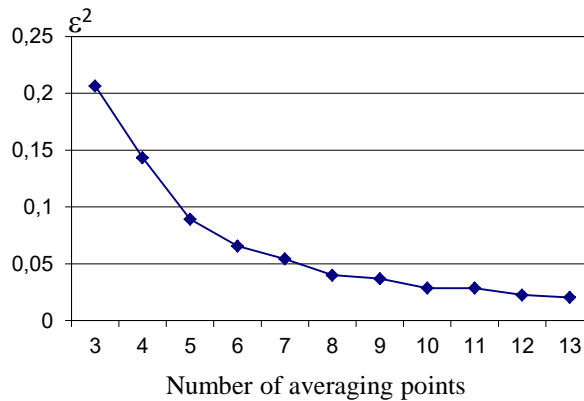


Fig. 7. The error of width estimation against the number of averaging points for the signal-to-noise ratio of 25.

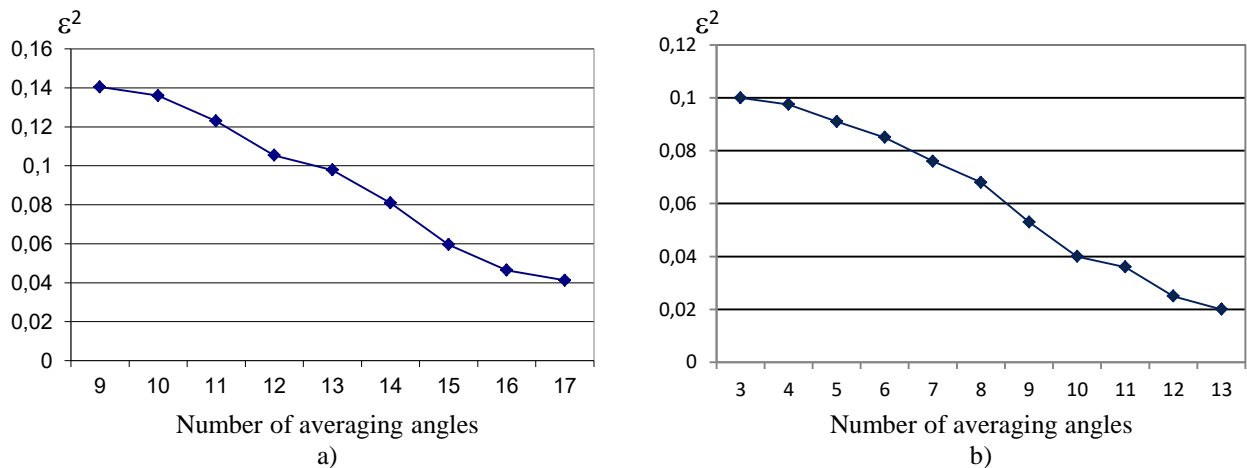


Fig. 8. The error of width estimation against the number of averaging angles given the signal-to-noise ratio of (a) 25 and (b) 15.

Figure 8 shows the diameter estimation error against the number of averaging angles (scanning sector size) with the r.m.s. signal-to-noise ratio, respectively, equal to 15 and 25. The experimental study showed that the greater is the volume of data used for averaging, the more reliably is the width estimation due to additional filtering of noise.

The experimental study showed that the estimation error can be essentially reduced by performing the averaging over a designated circumference sector of a local fan transform. As a disadvantage, we can mention that this approach is sensible to the highly curved vessels and the inability of the algorithm to be adjusted to the vessel and background brightness.

The directions were evaluated in a noisy 1024 x 1024 image (Fig. 9) with bifurcations uniformly located along the x-and y-axes. The general number of objects was 2,304.

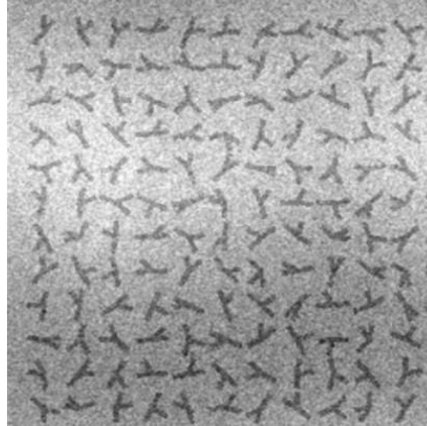


Fig. 9. Noisy test image.

A comparative study of the following methods for vessel direction and bifurcation identification was conducted: a direct method for direction identification (KM method), a method of a local discrete Radon transform, a method of a local discrete fan transform (LDFT) and a modified LFT [2]. The worst results were demonstrated by the algorithm based on the Radon transform variance estimation, because a classical Radon transform is unable to discern two opposite directions, thus leading to numerous cases of false recognition and the increased number of missed-out objects.

Table 1. Results of bifurcation detection using different techniques.

Method	Number of correctly recognized objects	Number of missed objects	Number of falsely recognized objects	General number of falsely recognized objects
KM method	2221	83	403	486
Discrete LRT	2016	288	192	480
LRT variance estimate	1812	492	235	727
MLFT method	2257	47	65	112
DLFT method	2240	64	222	286

The analysis showed that compared to other methods, the MLFT provides the least error of bifurcation angle estimation and the least error of false bifurcation recognition, is able to recognize correctly a larger proportion of bifurcations and the most stable to white noise.

6. Conclusion

Estimation of local blood vessel parameters used to form diagnostic features is a major problem of modern medicine, enabling an early diagnosis of various vascular pathologies. In this work, we have proposed a method for vessel diameter measurement that exploits a local fan transform. The method is based on the Radon transform, which is modified in such a way that bifurcations, crossovers, and terminations of vessels can be efficiently analyzed in the presence of interfering factors, including spots and close vessels. By analyzing the average brightness and variance of the radial function against the angle, vessel's width and direction can also be estimated and bifurcation points identified. To enhance the robustness, the transform is performed for a range of radii. The developed algorithm is stable to noise and disturbances, enabling bifurcations, crossovers, and terminations of vessels to be analyzed with high efficiency in the presence of interfering factors. The results of experiments have been discussed, showing in which way the accuracy of vessel width estimation is affected by the noise-to-signal ratio in the image under analysis, the vessel curvature, and the number of points and angles of averaging. The proposed method has been experimentally confirmed to be stable to various types of image noise.

The worst results have been shown by the estimation technique based on the Radon transform variance estimation because a classical Radon transform is unable to discern between two opposite directions, leading to a large number of false identifications and increased number of missed objects.

Acknowledgements

This work was partially supported by the Ministry of education and science of the Russian Federation in the framework of the implementation of the Program of increasing the competitiveness of SSAU among the world's leading scientific and educational centers for 2013-2020 years; by the Russian Foundation for Basic Research grants (# 15-29-03823, # 15-29-07077, # 16-41-630761; # 16-29-11698); by the ONIT RAS program # 6 "Bioinformatics, modern information technologies and mathematical methods in medicine" 2016 -2017.

References

- [1] Partha Sarathi M, Dutta Malay Kishore, Singh Anushikha, Travieso CM. Blood vessel inpainting based technique for efficient localization and segmentation of optic disc in digital fundus images. *Biomedical Signal Processing and Control* 2016; 108–117.
- [2] Ilyasova NYu, Kupriyanov AV, Khramov AG. Information technologies of image analysis in medical diagnostics. M.: Radio I Svyazj, 2012; 424 p.
- [3] Astakhov YS, Krasavina MI, Grigoryeva NN. Modern approaches to the treatment of a diabetic macular edema. *Ophthalmologic sheets* 2009; 59–69.
- [4] Pedersen L, Grunkin M, Ersbøll B, Madsen K, Larsen M, Christoffersen N, Skands U. Quantitative measurement of changes in retinal vessel diameter in ocular fundus images. *Pattern Recognition Letters* 2000; 1215–1223.
- [5] Ilyasova N. Methods for digital analysis of human vascular system. literature review. *Computer Optics* 2013; 37: 517–541.
- [6] Ilyasova N. Computer Systems for Geometrical Analysis of Blood Vessels Diagnostic Images. *Optical Memory and Neural Networks (Information Optics)* 2014; 23(4): 278–286.
- [7] Kupriyanov AV, Ilyasova NYu, Ananin MA, Malapheev AM, Ustinov AV. Evaluation of the geometric parameters of the optic nerve region on the images of the fundus. *Computer Optics* 2005; 28: 136–139.
- [8] Ilyasova N. Estimation of Geometric Characteristics of the Spatial Structure of Vessels. *Pattern Recognition and Image Analysis* 2015; 25(4): 621–625.
- [9] Ilyasova NYu. Evaluation of geometric features of the spatial structure of blood vessels. *Computer Optics* 2014; 38(3): 529–538.
- [10] Ilyasova NYu, Kupriyanov AV, Paringer RA. The Discriminant Analysis Application to Refine the Diagnostic Features of Blood Vessels Images. *Optical Memory & Neural Networks (Information Optics)* 2015; 24(4): 309–313.
- [11] Kupriyanov AV, Ilyasova NYu. Development of information technology for estimation of geometrical parameters of the image of the fundus. *Bulletin of the Samara State Aerospace University. Academician of SP Korolev (National Research University)* 2008; 2.
- [12] Fathi A, Naghsh-Nilchi AR. Automatic wavelet-based retinal blood vessels segmentation and vessel diameter estimation. *Biomedical Signal Processing and Control* 2013; 71–80.
- [13] Elaheh I, Malihe J, Hamid-Reza P. Improvement of retinal blood vessel detection using morphological component analysis. *Computer Methods and Programs in Biomedicine* 2015; 263–279.
- [14] Konstantinos K, Aristides I, Tsonos C, Assimakis N. Automatic model-based tracing algorithm for vessel segmentation and diameter estimation. *Computer Methods and Programs in Biomedicine* 2010; 108–122.
- [15] Lupas A, Tegolo D, Trucco E. Accurate estimation of retinal vessel width using bagged decision trees and an extended multiresolution Hermite model. *Medical Image Analysis* 2013; 1164–1180.
- [16] Gao X, Bharath A, Stanton A, Hughes A, Chapman N, Thom S. Measurement of vessel diameters on retinal images for cardiovascular studies. *On-line Conference Proceedings: Medical Image Understanding and Analysis* 2001; 123–135.
- [17] Gao XW, Bharath A, Stanton A, Hughes A, Chapman N, Thom S. Quantification characterisation of arteries in retinal images. *Computer Methods and Programs in Biomedicine* 2000; 63(2): 133–146.
- [18] Cai Menga, Jun Zhang, Fugen Zhou, Tianmiao Wang. New method for geometric calibration and distortion correction of conventional C-arm. *Computers in Biology and Medicine* 2014; 52: 49–56.
- [19] Ilyasova NYu, Kazanskiy NL, Korepanov AO, Kupriyanov AV, Ustinov AV, Khramov AG. Computer technology for reconstructing the 3D structure of coronary arteries from angiographic projections. *Computer Optics* 2009; 33(3): 281–318.
- [20] Moravec J, Hub M. Automatic correction of barrel distorted images using a cascaded evolutionary estimator. *Information Sciences* 2016; 366: 70–98.